Electronic Supplementary Material (ESI) for Journal of Materials Chemistry A.

Supplementary Information

Ultra-selective defect-free interfacially polymerized molecular sieve thin-film composite membranes for H_2 purification

*Zain Ali, Federico Pacheco, Eric Litwiller, Yingge Wang, Yu Han and Ingo Pinnau**

Advanced Membranes & Porous Materials Center, King Abdullah University of Science and Technology, Division of Physical Sciences and Engineering, Thuwal 23955-6900, KSA.

*ingo.pinnau@kaust.edu.sa

1. Experimental

1.1. Materials

m-Phenylenediamine (MPD, 99%) and trimesoyl chloride (TMC, 98%) were purchased from Aldrich. TMC was vacuum distilled at 110 °C before use and stored in a desiccator. Thin-film composite membranes were prepared on porous polysulfone (PS) ultrafiltration supports provided by Sepro Inc. (Carlsbad, CA, USA). The support was composed of a 50-µm-thick polysulfone membrane resting on a thick (100 µm) macroporous polyester layer. Isoparaffin G (Isopar®) was obtained from ExxonMobil and stored with 4 Å molecular sieves to prevent dissolution of atmospheric moisture. Before use, the solvent was further filtered using a 0.2 µm Teflon mesh. Isopropanol, 99.5+% ACS reagent, was purchased from Sigma Aldrich. Deionised water (DIW) was obtained from a Millipore Advantage A10 system. FT-30-type (RO4) commercial reverse osmosis membranes were purchased from Sepro Inc. Test gases, i.e. helium, hydrogen, oxygen, nitrogen, methane and carbon dioxide, were obtained from Specialty Gas Center (SGC), with purities > 99.99%.

1.2. Gas permeation measurements

Fig. S1 shows the custom-made thin film pure-gas permeation setup used. The system is based on the constant pressure/variable volume method. A Millipore stainless steel cell (active area 13.6 cm^2) was connected to a feed, permeate and retentate line. Membrane coupons were cut using an EPILOG mini laser cutter and sealed in the cell. Standard tests were performed at 22 °C.

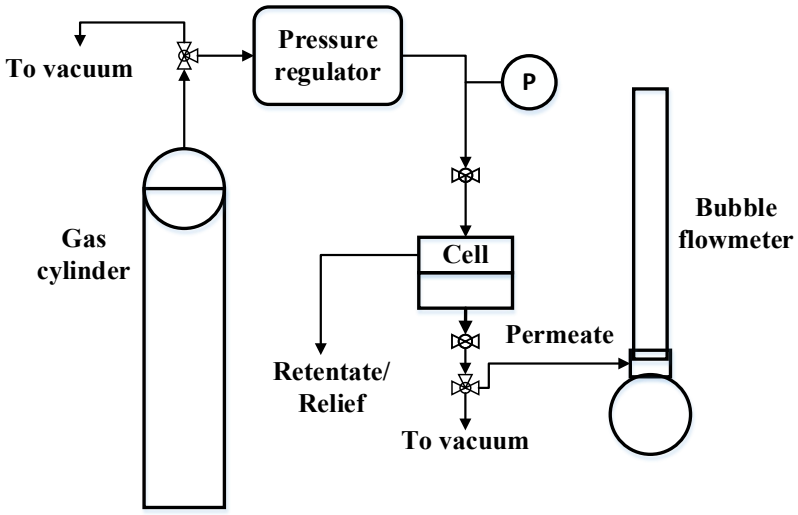

Fig. S1. *Pure-gas permeation system.*

Prior to the permeation test, both upstream and downstream were evacuated for 10 minutes. The feed gas was then loaded at 7.9 bar (100 psig). The permeate side of the membrane was exposed to atmospheric pressure (1 bar). Flow rates were measured using soap-bubble flow meters and the system was purged prior to the measurement with the respective test gas.

Permeance was calculated using the following equation;

$$Permeance = \frac{273 p_{atm} dV}{A(p_{feed} - p_{perm}) T 76 dt} \qquad \text{(Eq. 1)}$$

where p_{atm}, p_{feed} and p_{perm} are atmospheric, feed and permeate pressures (cmHg), respectively, dV/dt is the volumetric flow rate ($cm^3\ s^{-1}$), and T is the measurement temperature (K). Permeance was calculated in GPU where 1 GPU = 10^{-6} cm^3 (STP) cm^{-2} s^{-1} $cmHg^{-1}$.

Pure-gas selectivity (α) for each gas pair was calculated using the following equation:

$$\alpha_B^A = \frac{Permeance_A}{Permeance_B} \quad \text{(Eq. 2)}$$

Prior to the specific gas permeation tests, compressed air was permeated through the samples at 7.9 bar (100 psig) for 48 hours to allow for potential membrane compaction. Gas permeation properties were measured in the order helium, hydrogen, oxygen, nitrogen, methane and carbon dioxide. Between each gas permeation test, the membrane cell was evacuated for 10 minutes.

1.3. Pure-gas temperature dependence measurements

For temperature dependence measurements, the membrane cell was heated using heating tape at the desired test temperature until equilibration. Permeate was collected at room temperature. Pure-gas temperature dependence was conducted between 22 - 140 °C at a feed pressure of 7.9 bar.

1.4. H_2/CO_2 mixed-gas high temperature permeation measurements

Fig. S2 shows the apparatus used for mixed-gas permeation experiments. Initially, CO_2 was permeated through the system for 30 minutes to ensure that all atmospheric air in the lines was removed. The preheat coil and cell heating elements were heated to 140 °C. H_2 feed was then initiated. Both gases were fed at 500 ml/min totaling to a cross-flow rate of 1000 ml/min with H_2:CO_2 composition of 50:50. Flow rate through the membrane was measured using a bubble flow meter and permeate composition was measured continuously using an Agilent Technologies 490 Micro gas chromatograph equipped with TCD detectors. The permeate was collected at room temperature.

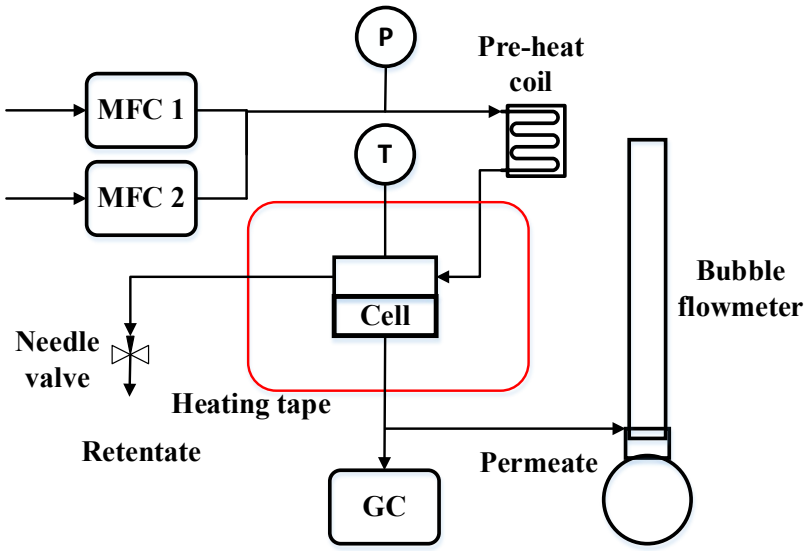

Fig. S2. *Mixed-gas permeation system.*

Separation factor was calculated as following:

$$Separation\ factor\ (\alpha) = \frac{xH_{2perm} / xH_{2feed}}{xCO_{2perm} / xCO_{2feed}} \quad \text{(Eq. 3)}$$

where xH_{2perm} and xH_{2feed} are the molar fractions of hydrogen in permeate and feed, respectively, and xCO_{2perm} and xCO_{2feed} are the molar fractions of carbon dioxide in permeate and feed, respectively.

Mixed-gas permeance in standard temperature/pressure (STP) for component *x* was calculated as:

$$Permeance = \frac{x_{perm} 273 p_{atm} dV}{A[(x_{feed}\, p_{feed}) - (x_{perm}\, p_{perm})]T76dt} \quad \text{(Eq. 4)}$$

where x_{perm} and x_{feed} are molar fractions of component x in permeate and feed, respectively.

1.5. Polymer powder synthesis

1 wt/vol% solutions of MPD (100 ml in distilled water) and 0.1 wt/vol% TMC (300 ml in Isopar®) were prepared separately and poured in a 1 L vial to begin the polycondensation reaction. The vial was rotated gently to ensure continuous interface generation. After 30 min, the polymer was removed and washed with 500 ml of Isopar® followed by vacuum filtration. The washing was repeated once with Isopar® followed twice with distilled water and twice with ethanol. After final filtration, the polymer was dried under vacuum at 120 °C for 20 h. Finally, the polymer was stored in a desiccator until further testing.

1.6. Membrane and polymer characterizations

To confirm presence of relevant functional groups on the surface of the TFCs, Fourier transform infrared (FTIR) spectroscopy was conducted using a Thermo Scientific Nicolet iS10 spectrometer. A germanium crystal was employed at an angle of 45° to obtain spectra between 4000 - 400 cm^{-1}. Chemical compositions of the surface of the TFCs were determined with a PHI-1600 (X-ray photoelectron spectroscopy) system using a penetration depth of 10 nm.

FEI Nova NanoSEM (Scanning Electron Microscope) was used for imaging of the surface and cross-sections of the membranes to examine structural features and layer homogeneity. Samples were sputter coated with iridium to improve conductivity. Samples for cross-sectional images were obtained by breaking the membrane following immersion in liquid N_2.

Wide-angle X-ray diffraction (XRD) pattern of the polyamide powder sample made from TMC and MPD was conducted on a Bruker D8 Advance diffractometer using a Bruker zero background sample holder at a scanning rate of 1° min^{-1}, 0.02° step size with 2θ ranging from 7° to 40° and the average chain spacing was calculated using Bragg's law. Thermal gravimetric

analysis (TGA, TA Q-5000) measurement of polyamide powder was carried out under nitrogen atmosphere with a drying step at 100 °C for 30 min followed by a ramp of 3 °C/min up to 800 °C.

2. USDOE requirements for hydrogen separation membranes

Table S1. *USDOE specified requirements for H_2/CO_2 membranes.*[1–3]

Low fabrication costs: approximately 100 USD/ft^2 or lower
Ability to manufacture large membrane areas and modules
High operating temperature: 120 – 150 °C and above
High pressure operability: 7 bar and above
High hydrogen purity and recovery
High durability: around 5 years
Performance: H_2 permeance > 200 GPU Mixed-gas H_2/CO_2 selectivity at 150 °C > 12 (IGCC operation)

3. MPD-TMC polymer structure

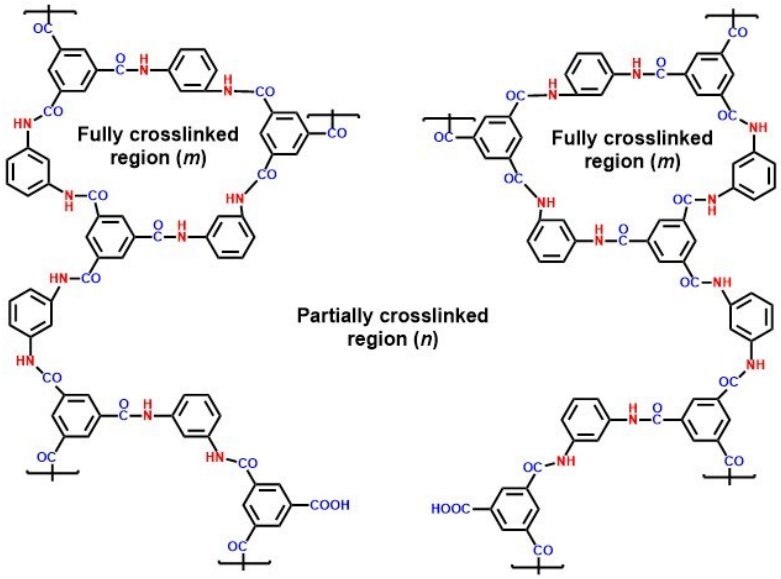

Fig. S3*. Aromatic polyamide structure via interfacial polymerization reaction between MPD-TMC.*[4]

4. In-situ micropore plugging process during long-term interfacial polymerization

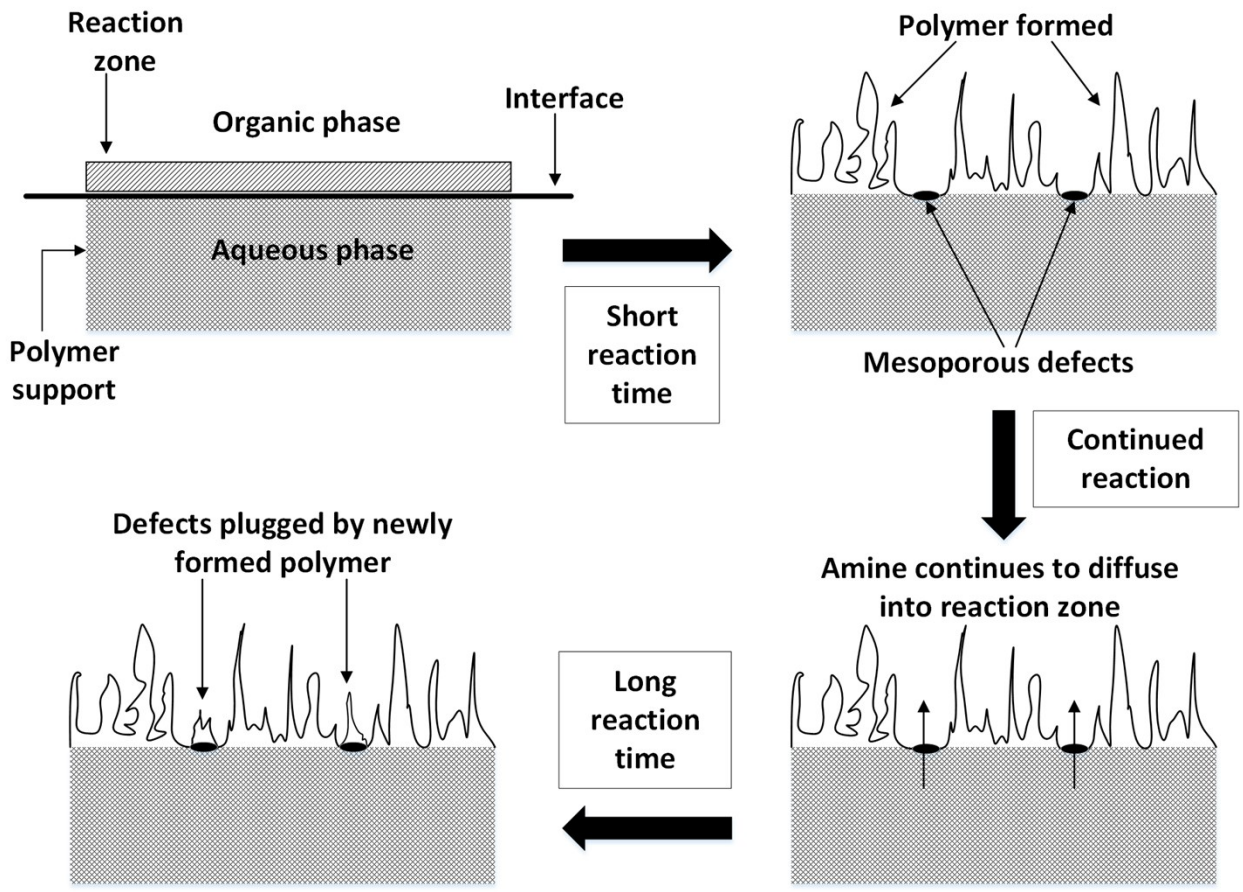

Fig. S4 *Proposed in-situ pore plugging process during long-term interfacial polymerization of thin-film composite membrane.*

5. Performance data

Table S2. *Gas permeance data (GPU = 1 x 10^{-6} cm^3(STP) cm^{-2} s^{-1} $cmHg^{-1}$) for prepared TFCs (T = 22 °C; Δp = 6.9 bar).*

Gas	FT-30-type RO-4	10s-0.1TMC-20C	60s-0.1TMC-20C	300s-0.1TMC-20C	600s-0.1TMC-20C	300s-0.1TMC-60C	300s-1TMC-60C	300s-10TMC-60C	300s-0.1TMC-100C
He	240.4	226.7	38.70	41.20	33.10	25.50	22.30	34.20	30.9
H_2	295.4	203.7	38.60	32.90	28.70	20.50	17.40	27.70	25.8
CO_2	106.2	67.6	7.60	4.30	4.60	1.10	1.50	2.90	1.80
O_2	87.4	60.0	4.10	1.10	1.40	0.30	1.00	2.00	0.40
N_2	91.0	69.2	3.90	0.60	0.90	0.06	0.80	1.80	0.04
CH_4	118.2	109.9	4.90	0.70	1.10	0.05	1.20	2.50	0.02

Table S3. *Gas pair selectivity data for prepared TFCs (T = 22 °C; Δp = 6.9 bar).*

Gas pair	FT-30-type RO-4	10s-0.1TMC-20C	60s-0.1TMC-20C	300s-0.1TMC-20C	600s-0.1TMC-20C	300s-0.1TMC-60C	300s-1TMC-60C	300s-10TMC-60C	300s-0.1TMC-100C
H_2/CO_2	2.80	3.00	5.10	7.60	6.20	18.9	12.0	9.50	14.3
H_2/N_2	3.30	3.00	10.1	59.5	30.6	328	20.8	15.0	644
H_2/CH_4	2.50	1.90	9.00	44.2	25.7	414	14.2	11.1	1380
O_2/N_2	1.00	0.90	1.10	2.00	1.50	5.20	1.20	1.10	8.70
CO_2/CH_4	0.90	0.60	1.60	5.80	4.10	22.0	1.20	1.20	96.8
N_2/CH_4	0.70	0.60	0.80	0.70	0.80	1.30	0.70	0.70	2.20
CO_2/N_2	1.20	1.00	2.00	7.90	4.90	17.4	1.70	1.60	45.1

6. FTIR spectra

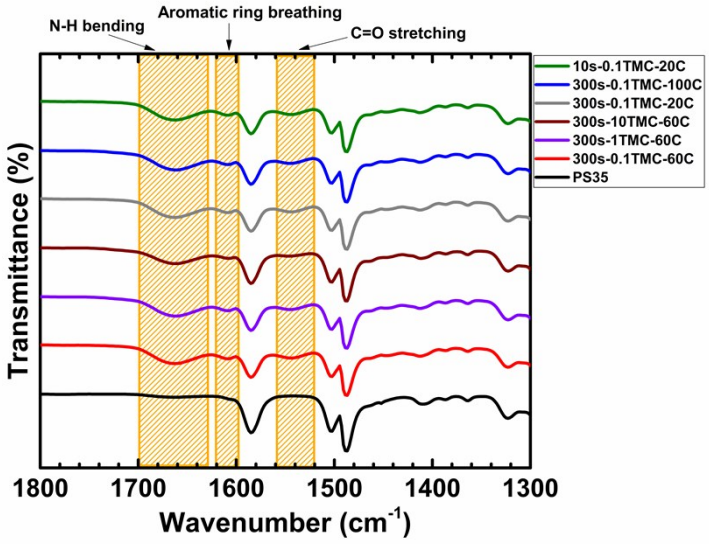

Fig. S5. *FTIR spectra for polysulfone and TFCs in this study.*

Fig. S5 shows the FTIR spectra of the TFCs along with bare polysulfone support. After the interfacial polymerization (IP) reaction, three new peaks appear. The peaks at 1545 cm^{-1} and 1660 cm^{-1} confirm the presence of amide groups on the surface of the composite membrane. The former relates to the C=O stretching while the latter corresponds to N-H bending in the amide linkage. The peak at 1610 cm^{-1} is associated with aromatic ring breathing.[5–7] Because the penetration depth of the IR beam was > 0.3 μm, the spectra of the polysulfone was clearly visible even after the support was coated with interfacially polymerized polyamide.[8]

7. X-ray diffraction (XRD)

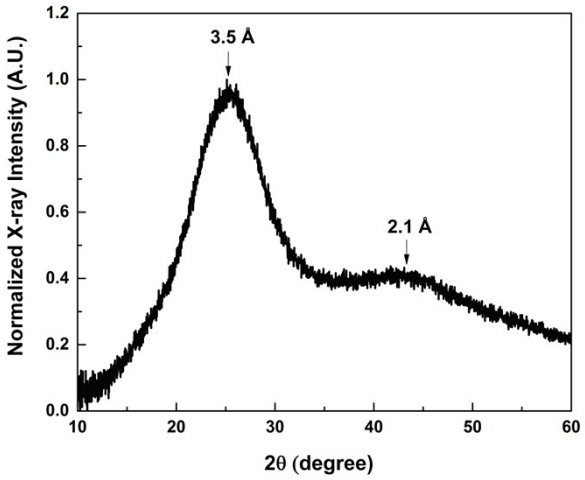

Fig. S6. *XRD data for polyamide powder prepared by interfacial polymerization of trimesoyl chloride and m-phenylenediamine.*

8. X-ray photoelectron spectroscopy (XPS)

Table S4*. XPS data for relevant fabricated TFCs.*

Membrane	C (%)	O (%)	N (%)	N/O	M
300s-0.1TMC-20C	76.0	13.5	10.5	0.78	0.62
300s-0.1TMC-60C	76.0	13.4	10.7	0.79	0.66
300s-1TMC-60C	76.5	13.5	10	0.74	0.55
300s-10TMC-60C	76.2	14.3	9.5	0.66	0.39
300s-0.1TMC-100C	77.5	11.7	10.9	0.93	0.89

XPS measurements were performed to obtain information about the chemical surface composition of the TFCs. Relative atomic concentrations and degree of cross-linking were determined using the method described by Kim et. al.[9] '*m*' describes the relative fractions of fully cross-linked regions in the polymer film (see Fig. S3).

9. TFC gas pair selectivity for alternative applications

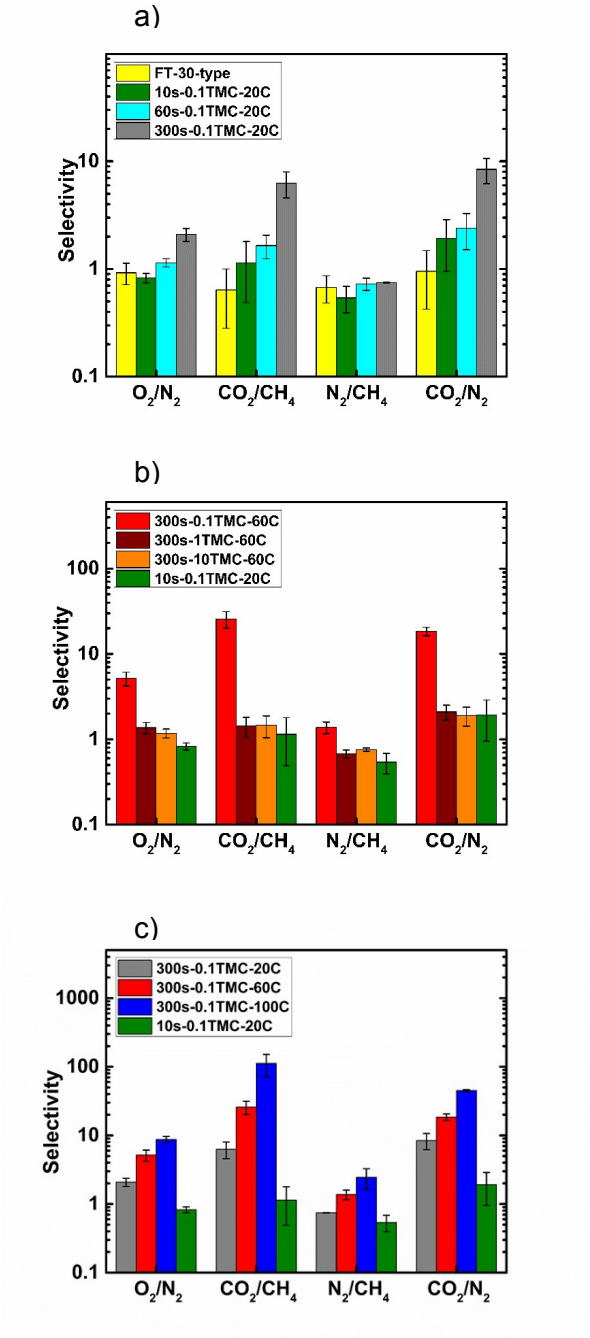

Fig. S7. O_2/N_2, CO_2/CH_4, N_2/CH_4 and CO_2/N_2 selectivity data for fabricated TFCs: a) reaction time variation, b) TMC concentration variation and c) organic phase temperature variation.

10. Field emission scanning electron microscopy (FESEM)

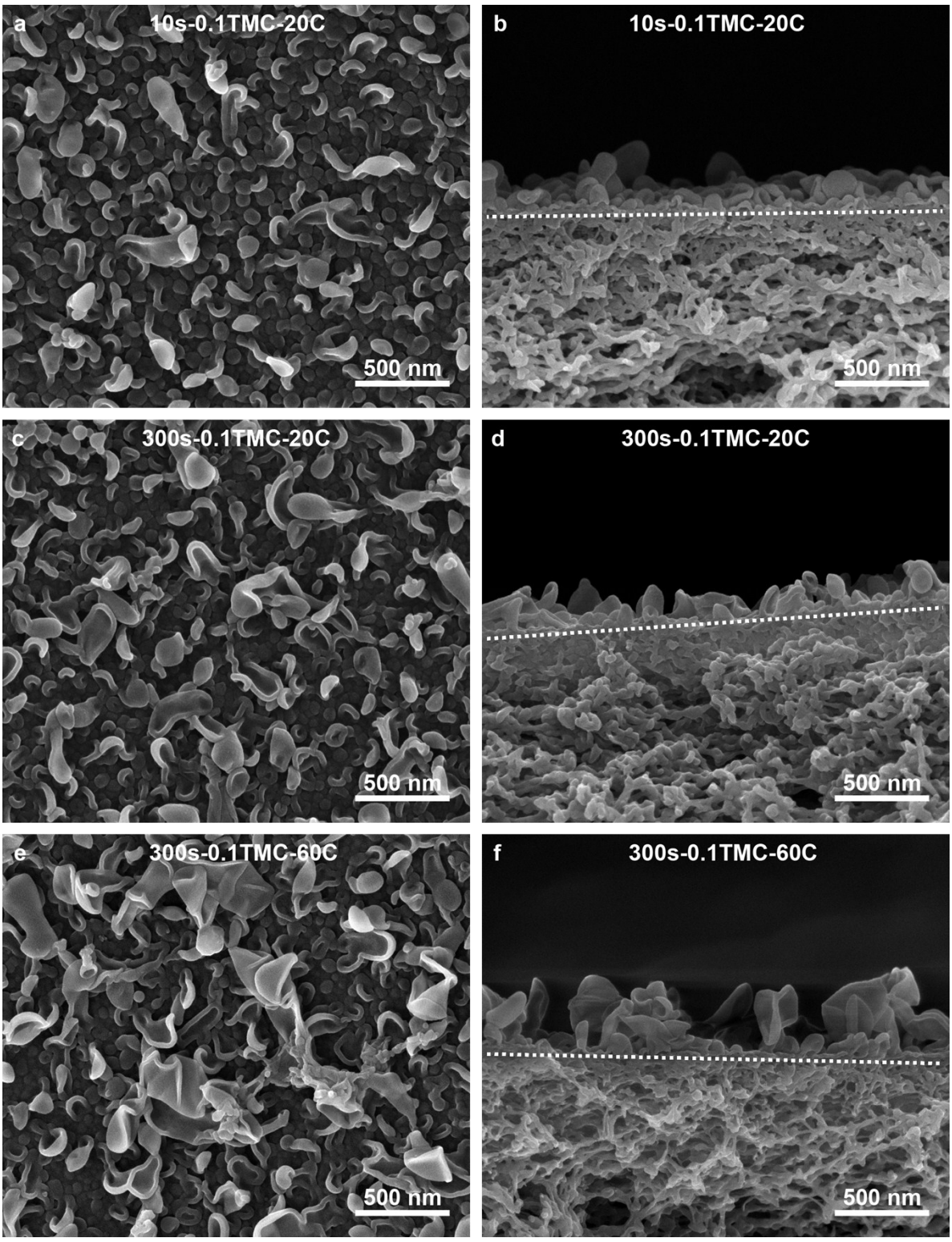

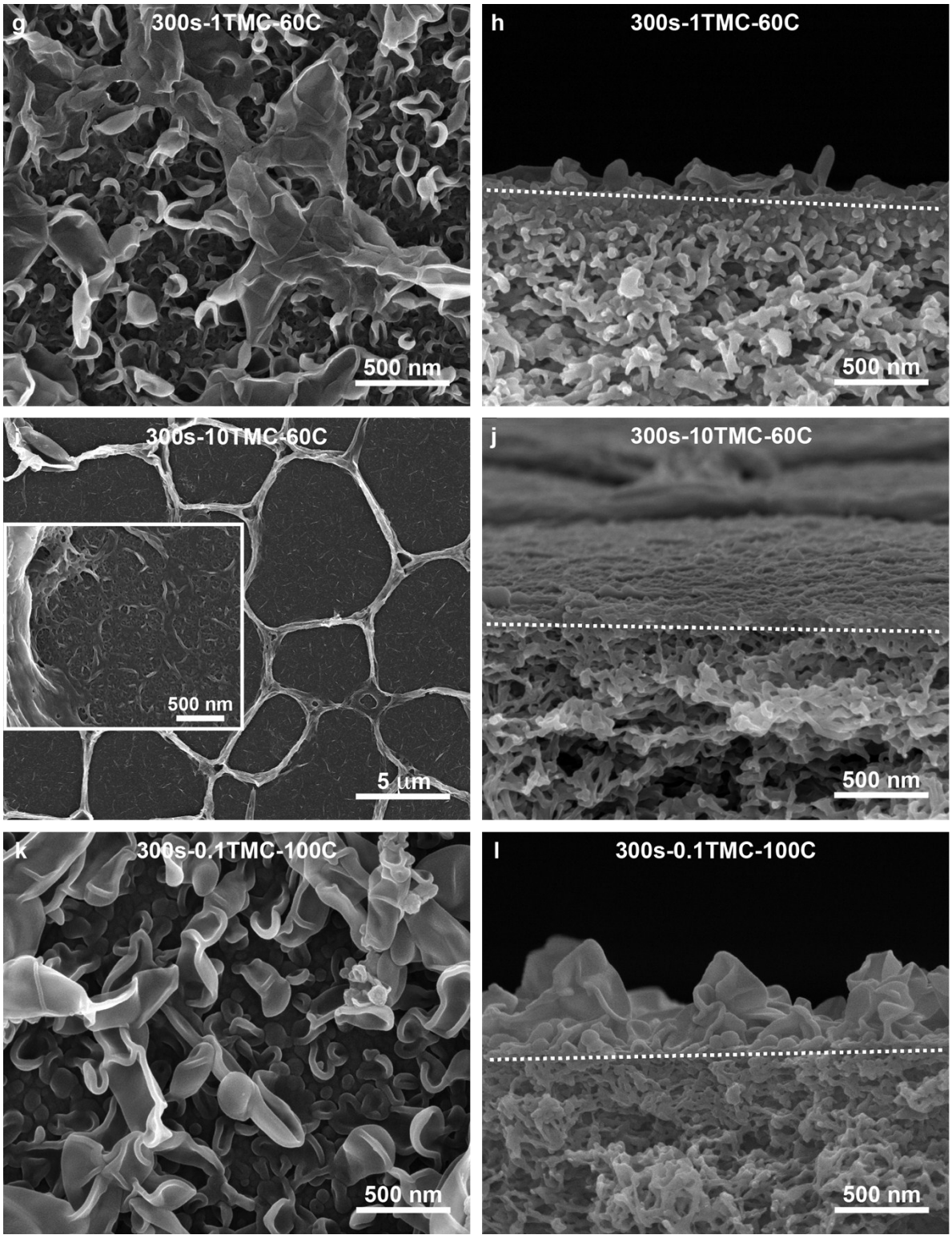

Fig. S8 *Top surface (a, c, e, g, i, k) and cross-section (b, d, f, h, j, l) FESEM images of fabricated TFCs.*

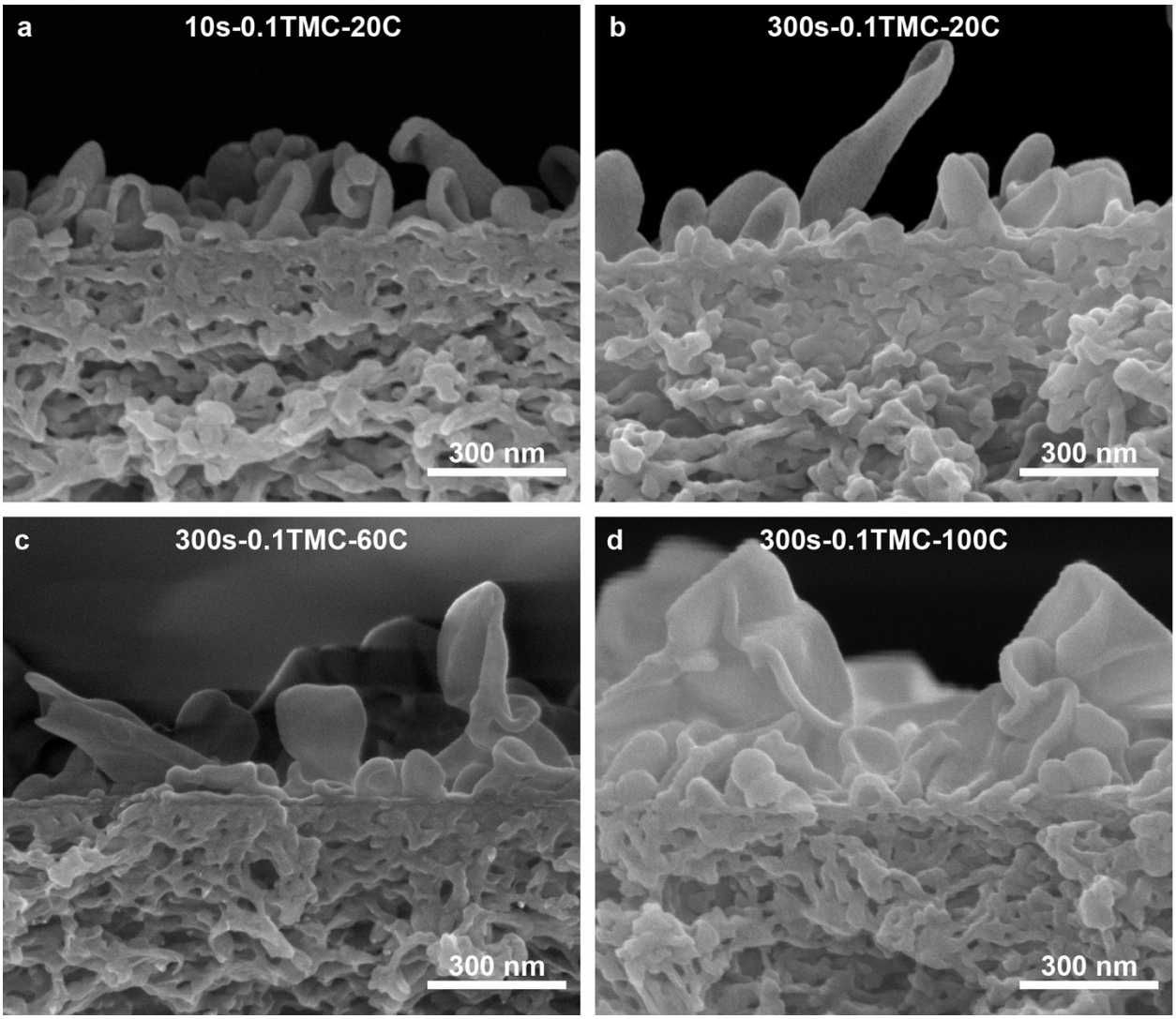

Fig. S9 *High magnification cross-section FESEM images of fabricated TFCs.*

11. Activation energy of permeation

The temperature dependence of gas permeance can be described as:

$$P = P_0 exp\left(\frac{-E_p}{RT}\right) \quad \text{(Eq. 5)}$$

where P_0 is a constant, E_p is activation energy of permeation (J mol^{-1}), R is the universal gas constant (8.314 J mol^{-1} K^{-1}) and T is the temperature (K).

E_p for each gas was calculated using the slope of log P plotted versus 1/T as in Fig. 3 (a).

12. Thermal gravimetric analysis

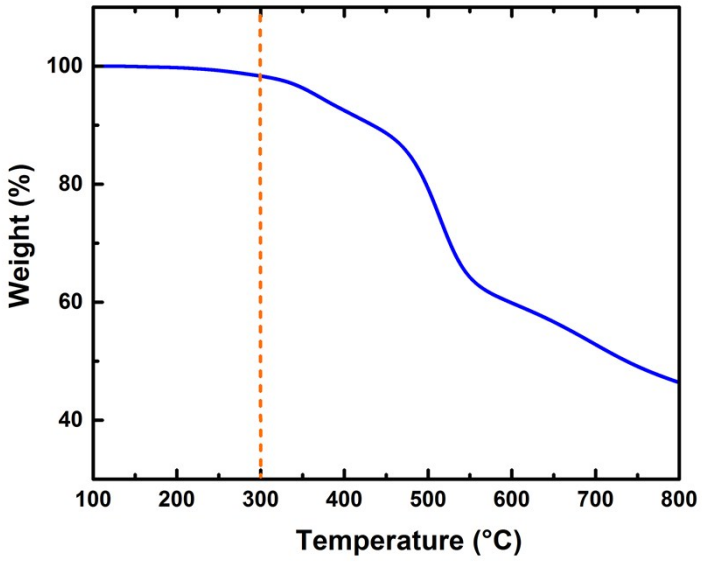

Fig. S10 *Thermal stability of polyamide powder sample made from trimesoyl chloride and m-phenylenediamine determined by TGA.*

13. References

1 United States Department of Energy, *Advanced Carbon Dioxide Capture R&D Program: Technology Update: Pre-combustion membranes*, Pittsburgh, 2013.

2 United States Department of Energy, *Basic research needs for the hydrogen economy. Workshop on hydrogen production, storage and use*, Lemont, 2003.

3 N. W. Ockwig and T. M. Nenoff, *Chem. Rev.*, 2007, **107**, 4078–4110.

4 J. Duan, PhD thesis, King Abdullah University of Science and Technology, 2014.

5 B. Khorshidi, T. Thundat, B. A. Fleck and M. Sadrzadeh, *RSC Adv.*, 2015, **5**, 54985–54997.

6 M. Liu, D. Wu, S. Yu and C. Gao, *J. Membr. Sci.*, 2009, **326**, 205–214.

7 Y. Jin, W. Wang and Z. Su, *J. Membr. Sci.*, 2011, **379**, 121–130.

8 A. P. Rao, S. V. Joshi, J. J. Trivedi, C. V. Devmurari and V. J. Shah, *J. Membr. Sci.*, 2003, **211**, 13–24.

9 S. H. Kim, S. Y. Kwak and T. Suzuki, *Environ. Sci. Technol.*, 2005, **39**, 1764–1770.